Unusual mesomorphic behaviour in bent-core compounds derived from 5-cyanoresorcinol

R. Amaranatha Reddy[a]; B. K. Sadashiva Corresponding author[a]

[a] Raman Research Institute, Bangalore-560 080, India

PLEASE SCROLL DOWN FOR ARTICLE

Unusual mesomorphic behaviour in bent-core compounds derived from 5-cyanoresorcinol

R. AMARANATHA REDDY and B. K. SADASHIVA*

Raman Research Institute, C. V. Raman Avenue, Sadashivanagar,
Bangalore-560 080, India

We describe the synthesis and mesomorphic properties of the first two homologous series of bent-core compounds derived from 5-cyanoresorcinol. The lower homologues in both series show a normal B_1 phase, and the mesophase of higher homologues exhibits very unusual textures and electro-optical switching behaviour. The observation of spiral growth patterns under a polarizing microscope, and only layer reflections from X-ray diffraction studies for these homologues, suggests that this mesophase is different from a B_2 phase. This mesophase shows chiral domains of opposite handedness which can be identified from electric field experiments. Under a triangular-wave electric field, at lower voltages although the mesophase shows a ferroelectric type switching behaviour it is actually antiferroelectric in nature. The observation of helical structures and spontaneously formed chiral domains suggests that the mesophase is a variant of the B_2 phase.

1. Introduction

The origin of layer chirality caused by ferroelectric polar order and a tilt of bent-core (BC) molecules within the layer has helped in the establishment of a new sub-field of thermotropic liquid crystals namely, banana-shaped liquid crystals. The compensation of layer polarization produces a ferro- and/or an antiferroelectric banana mesophase. The mesophases thus obtained are in the form of either chiral conglomerates or racemic structures, in spite of the layer being chiral. These observations have stimulated systematic theoretical and experimental investigations of the phase structures. Several well characterized banana (B) phases have been reported and most of them have additional sub-phases [1–6]. In the biaxial smectic A (SmA_b) phase, the molecules should have a preferred direction within the layers leading to an optical biaxiality of the orthogonal phase, and such a phase has been observed in mixtures [7]. However, in the polar biaxial smectic A (SmAP) phase, the long axes of the BC molecules orient along the layer normal and the polarization lies along the narrow axes in the smectic plane. This mesophase has C_{2V} symmetry and such a structure has been observed in pure compounds [8, 9]. A monoclinic structure with C_2 symmetry, namely a SmCP phase (B_2) is often observed in which the molecular bow plane is tilted with respect to the layer

normal while the polarization still remains in the layer plane. The most fascinating and structurally complicated mesophase is B_7 [3], which possesses a chiral C_1 symmetry. One of the textural features exhibited by this phase is the growth of spiral structures in addition to various other two-dimensional patterns [3, 10]. The spiral growth domains have also been seen in a number of different systems [4, 11, 12–14] for which the symbol B_7 was assigned although the X-ray diffraction (XRD) data were different from those reported for this phase [3]. Interestingly however, textural variants and the XRD data are similar for this mesophase derived from 2-nitro- or 2-cyano-resorcinol [3, 14]. In addition, the B_7 phase exhibited by these materials shows two- or three-dimensional ordering of the molecules and no electro-optical switching.

A third type of biaxial smectic phase with a triclinic symmetry (chiral C_1), namely, SmC_G (G stands for general) was theoretically predicted by de Gennes [15] and is characterized by two tilt directions of the molecules with respect to the layer normal (none of them retain an orientation with respect to the layers). It has not been possible so far to observe this phase in calamitic liquid crystals. However, after the discovery of banana liquid crystals, Brand *et al.* [16], based on theoretical calculations, extended this phase structure to bent-core molecules and proposed eight possible diastereomeric structures for the SmC_G phase using a combination of two tilt directions. Due to the bent shape of the molecules, it has been possible to obtain a chiral polar SmC_G phase in banana liquid crystals. The

*Author for correspondence; e-mail: sadashiv@rri.res.in

anticlinic tilt of antiferroelectric or the synclinic tilt of ferroelectric arrangements in combination with *synleaning* or *antileaning* of the molecules produces four chiral diastereomeric structures. The remaining synclinic anti-ferroelectric or anticlinic ferroelectric tilt arrangement with *synleaning* or *antileaning* of the molecules generates four diastereomeric racemic structures. However, the first experimental observation of a SmC_G phase was made by Jakli *et al.* [17] in a binary mixture of banana-shaped compounds showing B_2 and B_7 mesophases. Later, careful experiments by Jakli *et al.* [18] and Eremin *et al.* [19] suggested that one of the compounds (labeled as B_7) in the mixture may actually show a SmC_G phase. In addition, Walba *et al.* [20] reported a SmC_G phase with triclinic symmetry based on electro-optical investigations and some studies on freely suspended films.

As pointed out by Jakli *et al.* [17] the B_2 phase has only an in-layer polarization component, and the equidistant circular smectic layers (fan-shaped texture) can satisfy this requirement. However, in the B_7 phase additional coiling of the filaments or ribbons indicate the existence of out-of-layer polarization. These are distinguishing features of B_2 and B_7 mesophases from the point of view of optical textures, and the latter could also be a SmC_G phase having a triclinic symmetry. However, the number of compounds shown to exhibit a SmC_G phase appears to be too limited for one to generalize the exact molecular structural features required for the occurrence of this mesophase.

In 1998, Weissflog *et al.* [3, 21] reported a bent-core compound derived from 5-cyanoresorcinol with no liquid crystalline phase. They also suggested that the cyano group substitution at the 5-position prevents the formation of any mesophase in such five-ring compounds [22]. Until now, there has been no report of a bent-core compound derived from 5-cyanoresorcinol exhibiting a mesophase. Herein, we report detailed synthetic procedures and the mesomorphic behaviour of two new homologous series of seven-ring compounds derived from 5-cyanoresorcinol. These are symmetrical seven-ring esters containing a fluorine substituent on the middle phenyl ring of the arms of the bent core as shown in the structure.
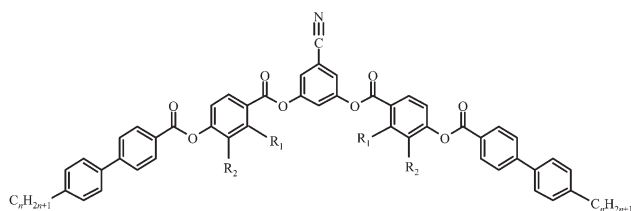
$n = 5, 6, \ldots\ldots 12, 14, 16, 18$

$R_1 = F, R_2 = H$ Series-**I**

$R_1 = H, R_2 = F$ Series-**II**

Structure.

2. Experimental
2.1. Synthesis

The synthesis of the two homologous series of compounds, composed of achiral symmetrical bent-core molecules containing a cyano substituent at the 5-position on the central phenyl ring and a fluorine substituent on the phenyl ring adjacent to it in the arms of the seven-ring esters, was carried out as shown in the scheme. 3,5-Dihydroxybenzonitrile [23] was obtained from 3,5-dimethoxybenzonitrile by demethylation using boron tribromide. The synthesis of 2-fluoro-4-benzyloxy-benzoic acid and 3-fluoro-4-benzyloxybenzoic acid have already been reported [24]. 4-*n*-Alkylbiphenyl-4-carboxylic acids were synthesized according to a procedure described earlier [25] and the transition temperatures obtained are consistent with literature values. The detailed synthetic procedure for one of the target compounds under investigation is given below.

2.1.1. *3,5-Dihydroxybenzonitrile, a*

A solution of 3,5-dimethoxybenzonitrile (3.0 g, 18.75 mmol) in anhydrous dichloromethane (20 ml) was cooled to $-70°C$ using liquid nitrogen. To this, a solution of boron tribromide (18.78 g, 75 mmol) in dichloromethane (20 ml) was added dropwise over a period of 1 h and the temperature was maintained for 2–3 h then allowed slowly to attain room temperature. The reaction mixture was then stirred for about 10 h at room temperature. Excess of boron tribromide was decomposed by the addition of moist chloroform. The mixture was then extracted with chloroform (2×50 ml) and the combined organic solution washed with water. Removal of solvent gave a solid material, which was passed through a column of silica gel using 5% acetone in chloroform as eluant. The light brown colour product obtained was crystallized from a minimum amount of water to give 3,5-dihydroxybenzonitrile; yield 1.9 g (79%), m.p. 190–192°C (reported [23] 164–170°C). ^{1}H NMR (acetone-d_6, 400 MHz) δ (ppm): 9.3 (s, 2H, $2 \times$ Ar–OH, exchangeable with D_2O), 6.8–6.79 (m, 2H, Ar–H, $^4J = 2.2$ Hz), 6.77–6.76 (m, 1H, Ar–H, $^4J = 2.1$ Hz). IR v_{max}: 3280, 2230, 1600 cm^{-1}. Elemental analysis: $C_7H_5O_2N$ requires C 62.22, H 3.73, N 10.37; found C 62.06, H 3.78, N 10.35%.

2.1.2. *5-Cyano-1,3-phenylene bis(3-fluoro-4-benzyloxybenzoate), c*

Compound **a** (1.35 g, 10 mmol) and 3-fluoro-4-benzyloxybenzoic acid, **b** (4.92 g, 20 mmol) were dissolved in anhydrous dichloromethane (50 ml). After the addition of *N,N′*-dicyclohexylcarbodiimide (DCC), (4.5 g, 22 mmol) and a catalytic amount of
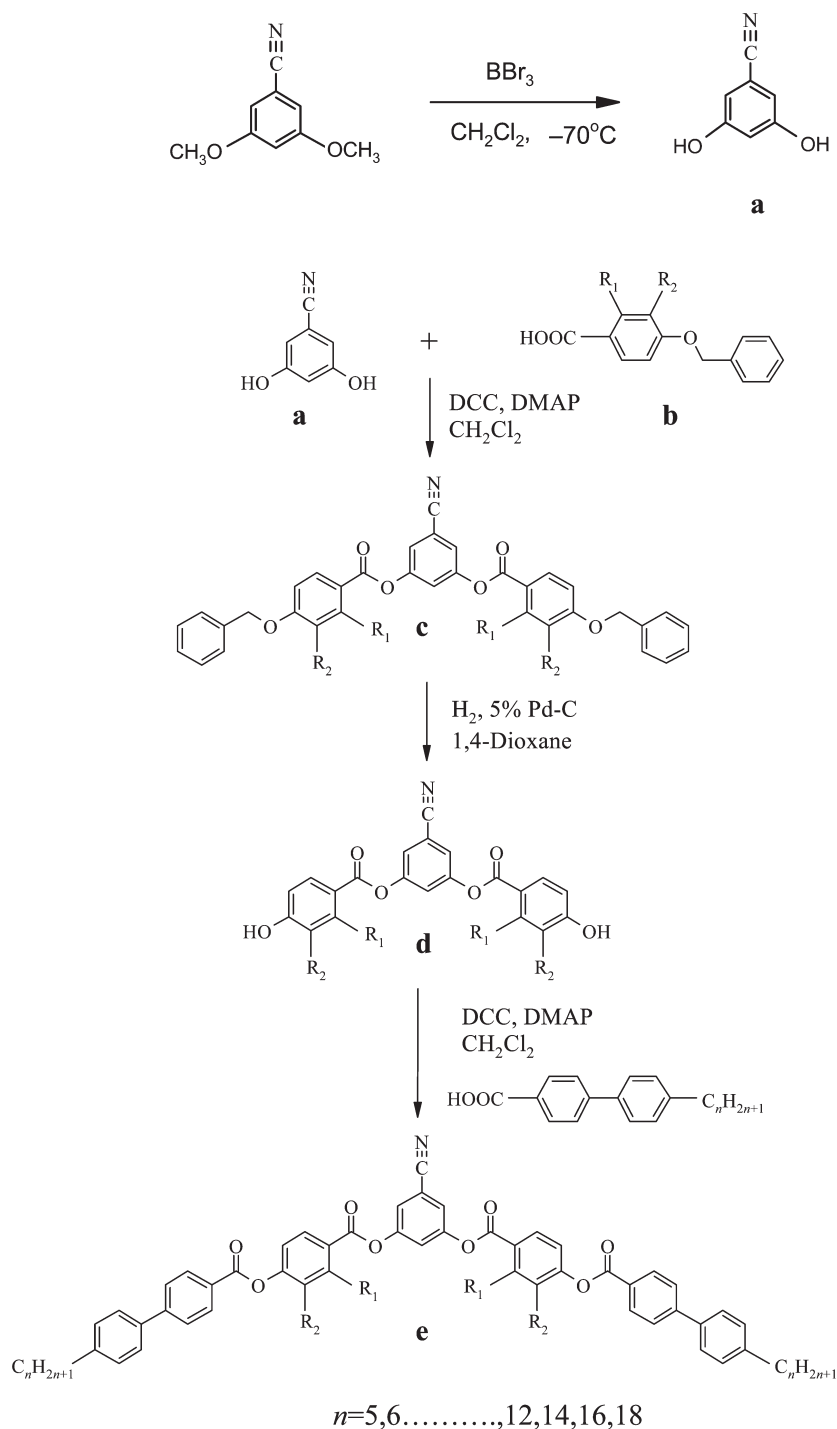
Scheme. General pathway used to synthesize the seven-ring symmetrical banana-shaped mesogens.

4-(*N*,*N*-dimethylamino)pyridine (DMAP), the mixture was stirred at room temperature for about 15 h. The dicyclohexylurea which precipitated was filtered off and washed with excess of chloroform (100 ml). The combined organic solution was washed with 2% cold aqueous acetic acid (3×50 ml) and 5% ice-cold sodium hydroxide solution (3×50 ml), then finally washed with water and dried (anhydrous Na_2SO_4). The solid material obtained after removal of solvent was chromatographed over silica gel and eluted using chloroform. Removal of solvent from the eluate afforded a white material, which was crystallized

from acetonitrile; yield 3.8 g (65%), m.p. 176–177°C. ^{1}H NMR (CDCl$_3$, 400 MHz) δ (ppm): 7.93–7.87 (m, 4H, Ar–H), 7.47–7.36 (m, 13H, Ar–H), 7.12–7.08 (m, 2H, Ar–H), 5.25 (s, 4H, 2 × ArCH$_2$O–). IR ν_{max}: 2228, 1745, 1728, 1612, 1591 cm^{-1}.

2.1.3. 5-Cyano-1,3-phenylene bis(3-fluoro-4-hydroxybenzoate), d

Compound **c** (3.5 g) was dissolved in 1,4-dioxane (40 ml) and 5% Pd-C catalyst (0.7 g) was added. The mixture was stirred at 50°C in an atmosphere of hydrogen until the required quantity of hydrogen was absorbed. The resultant mixture was filtered hot and the solvent removed under reduced pressure. The residue was passed through a column of silica gel and eluted using a mixture of 8% acetone in chloroform. Removal of solvent from the eluate gave a white material, which was crystallized from a mixture of butan-2-one and petroleum-ether (b.p. 60–80°C); yield 2.2 g (90%), m.p. 220–222°C. ^{1}H NMR (acetone-d$_6$, 400 MHz) δ (ppm): 10.25 (s, 2H, 2 × Ar–OH, exchangeable with D$_2$O), 8.06–8.02 (m, 4H, Ar–H), 7.907–7.902 (d, 2H, Ar–H, ^4J = 2.1 Hz), 7.85–7.84 (t, 1H, Ar–H, ^4J = 2.1 Hz), 7.36–6.31 (m, 2H, Ar–H). IR ν_{max}: 3333, 2233, 1745, 1718, 1618, 1595 cm^{-1}.

2.1.4. 5-Cyano-1,3-phenylene bis[4-(4-n-tetradecyl-biphenyl-4-carbonyloxy)-3-fluorobenzoate], 16

This was synthesized following a procedure similar to that given for compound **c.** Quantities: compound **d** (0.2 g, 0.486 mmol), 4-n-tetradecylbiphenyl-4-carboxylic acid (0.38 g, 0.973 mmol), DCC (0.22 g, 1 mmol), DMAP (cat. quantity), anhydrous CH$_2$Cl$_2$ (10 ml); yield 0.25 g (45%), m.p. 152°C. ^{1}H NMR (CDCl$_3$, 400 MHz) δ (ppm): 8.29–8.27 (d, 4H, Ar–H, ^3J = 8.4 Hz), 8.09–8.04 (m, 3H, Ar–H), 7.77–7.75 (d, 4H, Ar–H, ^3J = 8.4 Hz), 7.6–7.48 (m, 10H, Ar–H), 7.32–7.30 (d, 4H, Ar–H, ^3J = 8.1 Hz), 2.7–2.65 (t, 4H, 2 × Ar–CH$_2$–, ^3J = 7.5 Hz), 1.66–1.64 (quin, 4H, 2 × Ar–CH$_2$–CH$_2$, ^3J = 6.8 Hz), 1.34–1.26 (m, 44H, 22 × –CH$_2$–), 0.9–0.87 (t, 6H, 2 × –CH$_2$–CH$_3$, ^3J = 6.7 Hz). ^{13}C NMR (CDCl$_3$, 400 MHz) δ (ppm): 163.5, 162.6, 155.5, 153.0, 151.6, 150.4, 147.1, 143.7, 136.9, 131.1, 129.2, 127.2, 127.0, 126.5, 124.6, 123.2, 120.9, 119.0, 118.8, 116.9, 114.2, 45.2, 35.7, 31.9, 31.4, 30.9, 29.7, 29.5, 29.4, 22.7, 14.1. IR ν_{max}: 2247, 1748, 1736, 1608 cm^{-1}.

2.2. Characterization

Textural observations were made under a polarizing optical microscope (POM) (Leitz Laborlux 12 POL/Olympus BX 50) connected to a heating stage and a central processor (FP 82 HT and FP 90, respectively).

A differential scanning calorimeter (DSC) (Perkin-Elmer, Model Pyris 1D) was used to determine the transition temperatures and associated enthalpy changes of the mesophases under investigation. The mesophases obtained were identified by XRD measurements using a 4 kW rotating anode X-ray source (Rigaku Ultrax 18) with graphite crystal monochromated Cu Kα radiation (1.54 Å). The diffraction patterns of the unoriented samples were collected on an imaging plate (Marresearch). Polarization measurements were carried out using a triangular-wave method; triangular-wave voltages were generated from a waveform generator (Wavetek, Model 39), which was amplified using a TREK MODEL 601B-3 amplifier. The current response traces were recorded using a Tektronix Oscilloscope, TDS 220. The d.c. field switching characteristics were also obtained for some of the compounds using a regulated dual d.c. power supply (APLAB, Model LD6401).
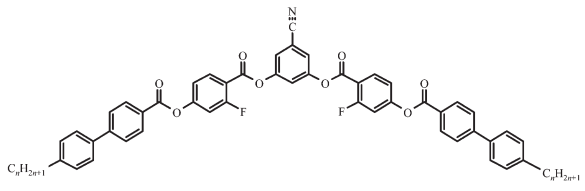
In order to confirm the chemical structure of the compounds synthesized, NMR (^{1}H and ^{13}C) spectra were recorded using a Bruker AMX 400 spectrometer (tetramethylsilane as an internal reference), the infrared spectra were obtained on a Shimadzu FTIR-8400 spectrophotometer. Elemental analysis was carried out using a Carlo-Erba 1106 analyser. All the target materials, as well as the intermediate compounds, were purified by column chromatography (silica gel, 60–120 mesh) and were crystallized using suitable analytical grade solvents. The purity of all these compounds was confirmed using normal phase high performance liquid chromatography (μ-Porasil column, 3.9 × 300 mm, Waters Associates Inc.) and using 1% acetone in dichloromethane as the eluant.

3. Results and discussion
3.1. Phase studies

The two homologous series of compounds, series **I** and **II**, differ only in the position of the fluorine substituent. In compounds of series **I**, a fluorine is substituted at the *ortho*-position while in series **II** it is at the *meta*-position with respect to the carboxylate group of the phenyl ring adjacent to the central phenyl ring. In both series of compounds only two kinds of mesophases were observed. The transition temperatures and associated enthalpy changes obtained for compounds of series **I** and **II** are summarized in tables 1 and 2, respectively. Looking first at the lower homologues of series **I**, on slow cooling of the isotropic liquid of compound **3**, dendritic patterns develop which coalesce to form a mosaic texture. Spherulitic growth could sometimes also be seen, which is a sign of a two-dimensional structure. These textural features point strongly towards a two-dimensional rectangular

Table 1. Transition temperatures (°C) and enthalpies (kJ mol^{-1}) (in italics) for compounds of series **I**. Key applicable to all the tables: Cr = crystalline phase; B$_{2X}$ = variant of a B$_2$ phase; B$_1$ = two-dimensional rectangular columnar phase; I = isotropic phase.
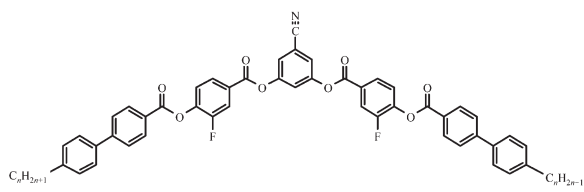

Compound	n	Cr		B$_{2X}$		B$_1$		I
1	5	●	177.5 *25.2*	—		●	216.0 *23.5*	●
2	7	●	179.0 *28.4*	—		●	206.0 *26.1*	●
3	8	●	182.0 *27.9*	—		●	195.5 *26.5*	●
4	9	●	189.0 *29.0*	—		●	192.0 *26.5*	●
5	10	●	189.5 *48.1*	—		—		●
6	11	●	183.5 *28.8*	●	188.0 *29.1*	—		●
7	12	●	178.0 *27.4*	●	188.0 *29.9*	—		●
8	14	●	172.5 *33.8*	●	188.5 *30.1*	—		●
9	16	●	166.5 *40.2*	●	188.0 *30.6*	—		●
10	18	●	161.0 *46.4*	●	187.0 *30.9*	—		●

Table 2. Transition temperatures (°C) and enthalpies (kJ mol^{-1}) (in italics) for compounds of series **II**.

Compound	n	Cr		B$_{2X}$		B$_1$		I
11	8	●	155.0 *19.9*	—		●	205.0 *25.5*	●
12	9	●	157.0 *19.9*	—		●	201.0 *27.4*	●
13	10	●	156.0 *22.1*	—		●	195.0 *27.4*	●
14	11	●	156.0 *23.9*	—		●	189.5 *27.5*	●
15	12	●	158.0 *30.3*	●	184.3[a]	●	184.5[a] *27.2*	●
16	14	●	152.0 *38.4*	●	184.0 *27.3*	—		●
17	16	●	145.0 *34.9*	●	182.0 *27.6*	—		●
18	18	●	141.5 *38.0*	●	181.0 *28.4*	—		●

[a]Enthalpy denoted is the sum of both the phase transitions.

columnar phase, namely a B$_1$ mesophase. Similar textural features were observed for compounds **1**, **2** and **4**. The clearing transition enthalpy value obtained for this mesophase is in the range 23–27 kJ mol^{-1}, and the corresponding melting transition enthalpy is in the range of 25–29 kJ mol^{-1}. This value increases gradually on increasing the *n*-alkyl chain length. Surprisingly, compound **5** is not liquid crystalline and this is the homologue where a cross-over from the B$_1$ to B$_{2X}$ (see later) phase occurs.

Similarly, the lower homologues of series **II** (compounds **11**, to **14**) also showed a mesophase similar to a

B$_1$ phase, whose melting and clearing enthalpy values were in the range 20–24 and 25–28 kJ mol^{-1} respectively. Both the melting and clearing transition enthalpies increase on ascending the series. The structure of the B$_1$ phase was further confirmed by XRD studies, which showed a rectangular lattice. The *d*-spacings and corresponding lattice parameter values obtained for compounds **2** and **11** are given in table 3; both compounds show a wide angle diffuse peak at about 4.8 Å indicating the fluidity of the alkyl chains in the mesophase.

The higher homologues of series **I** (compounds **6** to **10**) and **II** (compounds **15** to **18**) showed similar textural features which were completely different from the textures observed for the lower homologues. Compound **16** showed the following textural features.

Table 3. The measured *d*-spacings (Å) in the small angle region for the mesophases of various compounds.

Compound	*d*-spacings/Å (Miller indices)	Phase type	T/°C
2	27.4(1 1), 22.4(0 2); $a = 34.5$ Å, $b = 45$ Å	B$_1$	185
6	40.0 (0 1), 20.0 (0 2)	B$_{2X}$	184
8	42.9 (0 1), 21.4 (0 2), 14.3 (0 3)	B$_{2X}$	175
9	45.5 (0 1)	B$_{2X}$	170
11	31.7 (1 1), 23.5 (0 2); $a = 43$ Å, $b = 47$ Å	B$_1$	160
15	40.4 (0 1), 20.2 (0 2)	B$_{2X}$	165
18	52.0 (0 1), 26.0 (0 2), 17.3 (0 3), 13.0 (0 4)	B$_{2X}$	145
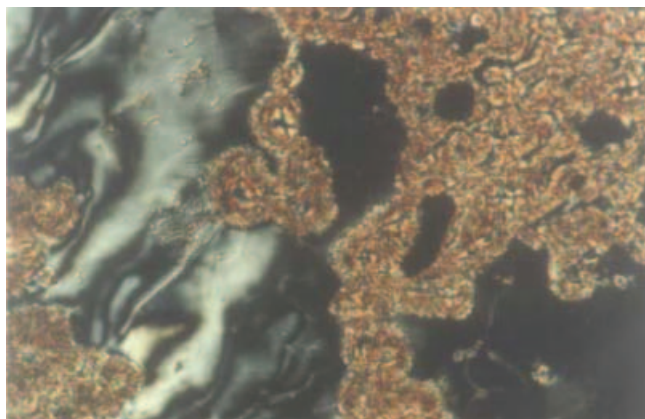
Figure 1. Optical photomicrograph of a B_{2X} phase texture obtained for compound **16**.
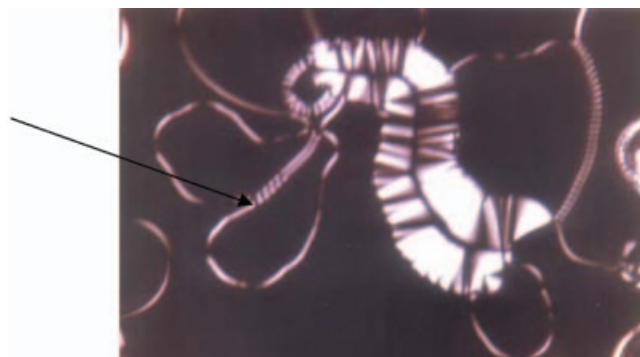

Figure 2. Optical photomicrograph of the growth of filaments from the isotropic phase of compound **16**. The transformation from a filamentary pattern to a helical pattern (as indicated by the arrow) can be seen.

Upon cooling the isotropic liquid, a schlieren texture with beaded filaments as well as a fingerprint pattern, which is normally seen for a B_2 phase, were obtained, as shown in figure 1. The appearance of the schlieren texture suggests an inhomogeneous in-plane orientation of the director field. However, on very slow cooling of the isotropic liquid, the mesophase grew as long filaments and coalesced to an undefined texture (bright); sometimes these filaments transformed to a helical pattern, see figure 2. In addition, short single-spiral helices could be seen to grow directly from the isotropic liquid. No other textural patterns were observed for these materials that are normally seen for a B_7 phase [3, 14]. Sometimes the mesophase exhibited circular domains in which the dark brushes were oriented parallel to the directions of the crossed polarizers (domain 1); in some other domains they rotated in clockwise (domain 2) and anticlockwise (domain 3) directions. A typical photomicrograph obtained for a homogeneously aligned cell (thickness

5.5 μm) showing these features is shown in figure 3. Some of these circular domains exhibit equidistant concentric stripes which are distinct features of a helical structure for the mesophase, see figure 4. This mesophase exhibits other very unusual textures, as shown in figures 2 and 5 (*a*). The schlieren texture obtained shows both $s = \pm 1/2$ and $s = \pm 1$ dark brushes as shown in figure 5 (*b*). This indicates an antiferroelectric ground state structure for the mesophase. Although the mesophase appears with some textural features of a B_2 phase, the additional complex textural patterns indicate that it could be a B_2 phase variant, which will be discussed later. Hence, this mesophase has been designated as a B_{2X} phase. Similar textural variants could be observed for the other homologues in the series. The clearing transition enthalpy value is rather high and increases from 29–31 kJ mol^{-1} on ascending the homologous series **I**. The corresponding melting enthalpy value is in the range 28–47 kJ mol^{-1}. Similarly, for series **II**, the clearing transition enthalpy increases
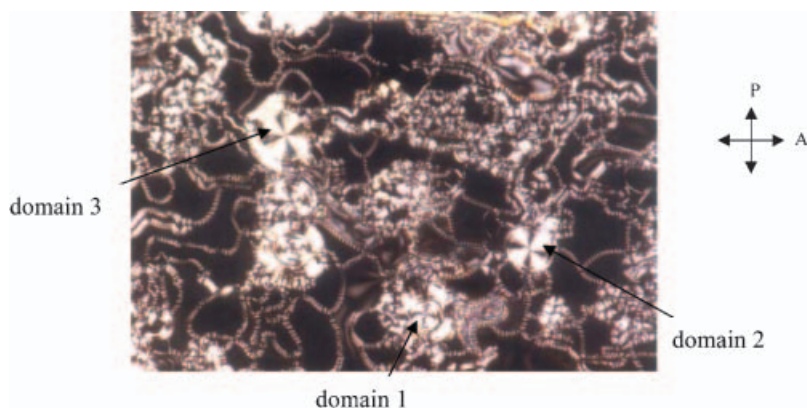

Figure 3. Optical photomicrograph obtained in a homogeneously aligned cell on cooling the isotropic liquid of a sample of compound **16**, showing single-wound helical pattern, circular domains and schlieren texture.
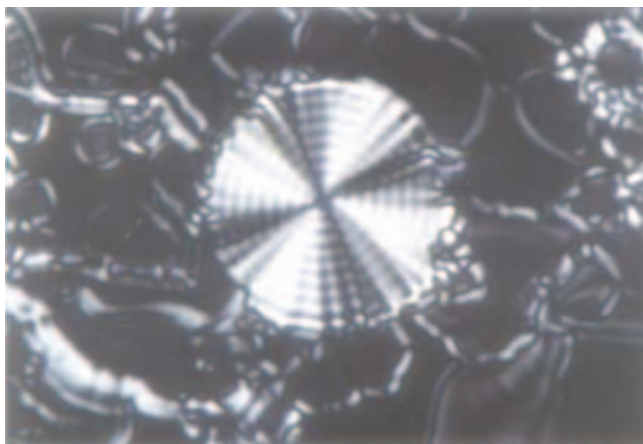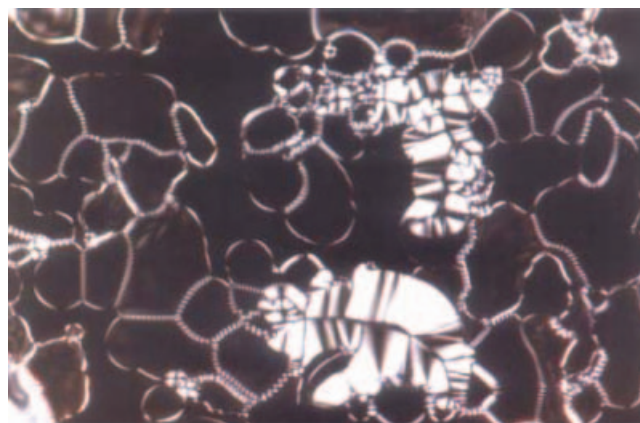
Figure 4. Optical photomicrograph showing a circular domain in which equidistant circular stripes are indicative of helical periodicity for the mesophase of compound **16**.

from 27 to 29 kJ mol^{-1} and the corresponding melting enthalpy value is in the range 30–38 kJ mol^{-1}. A DSC thermogram obtained for compound **16** is shown in figure 6. In addition to the B$_{2X}$ mesophase, many crystal–crystal transitions could be seen during heating and cooling.

An understanding of the occurrence of the filaments is a complex problem. Meyer *et al.* [26] reported a filamentary growth pattern at the I–SmA phase transition, and proposed that to negative interfacial surface tension anisotropy ($\Delta\gamma < 0$) is a necessary condition for the formation of filaments. $\Delta\gamma = \gamma_\| - \gamma_\perp$ where $\gamma_\|$ and $\gamma_\perp$ are the surface tensions for interfaces parallel and perpendicular to the smectic layers. For a number of systems $\Delta\gamma > 0$, but filaments can be produced only for those materials in which $\Delta\gamma < 0$. The surface tension associated with the interface between the isotropic liquid and mesophase is anisotropic (formation of filaments). On further cooling, the filaments transform to chiral helical structures as shown in figure 2. The transformation of filaments to helical structure is due to a phase transition from SmC$_S$P$_A$ to SmC$_A$P$_A$ structures on lowering the temperature.

Interestingly, only compound **15** exhibits two mesophases. On very slow cooling of a thin film sample to 182.5°C, mosaic as well as spherulitic textures were obtained, which are indicative of a two-dimensional B$_1$ phase. On further cooling to 182.3°C, along with the B$_1$ phase texture, schlieren texture and fingerprint patterns (normally seen for a B$_2$ phase) were observed. This indicates a phase transition from B$_1$ to a B$_{2X}$ phase. On further cooling, the B$_{2X}$ phase texture dominated but B$_1$ phase features could also be seen, see figure 7. However, no indication of such a transition could be
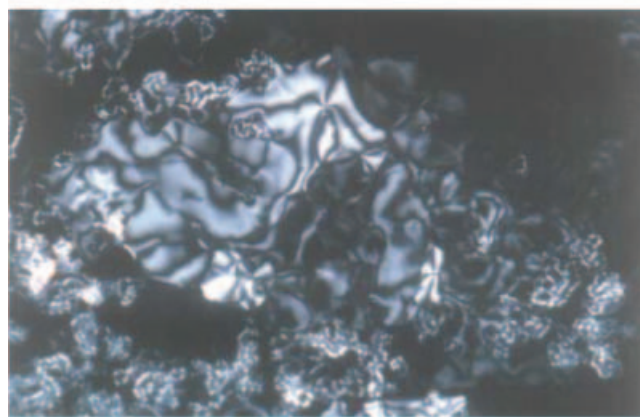
Figure 5. Optical photomicrographs showing (*a*) the appearance of a complicated textural pattern in which both helical as well as filamentary patterns are obtained on cooling the isotropic liquid of compound **16**; (*b*) a schlieren texture comprising both two- and four-brush defects for the same compound.
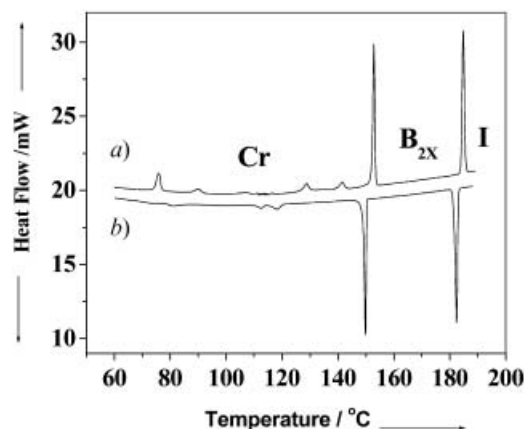

Figure 6. DSC thermogram obtained for compound **16**: (*a*) heating cycle, (*b*) cooling cycle; rate 5°C min^{-1}.
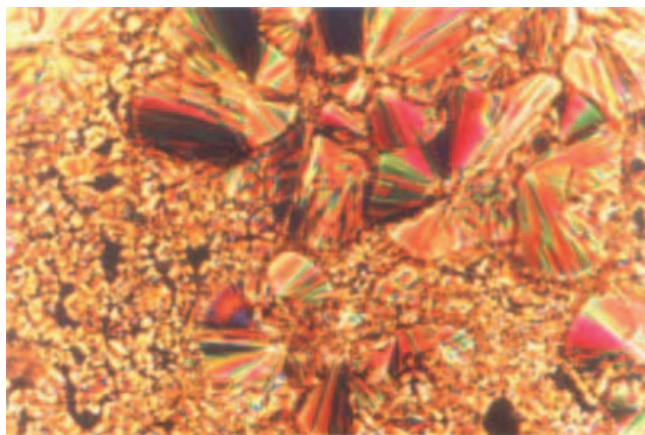
Figure 7. Optical photomicrograph showing the coexistence of both spherulites (B_1 phase) and the texture of a B_{2X} phase exhibited by compound **15**.

observed on a DSC thermogram and the enthalpy denoted in table 2 is the sum of both transitions.

In table 3, XRD data are given for five compounds exhibiting the B_{2X} mesophase, and suggest a tilted smectic phase. The calculated tilt angle is about 42–45°. In all these cases, a wide angle diffuse maximum is obtained at about 4.8 Å indicating the absence of in-plane order. The X-ray angular intensity profile obtained in the B_{2X} mesophase exhibited by compound **18** is shown in figure 8.

3.2. Electro-optic studies

Electro-optic studies were carried out on the mesophase of several compounds under investigation and in detail for compound **16**. The mesophase of this compound shows the following unusual switching
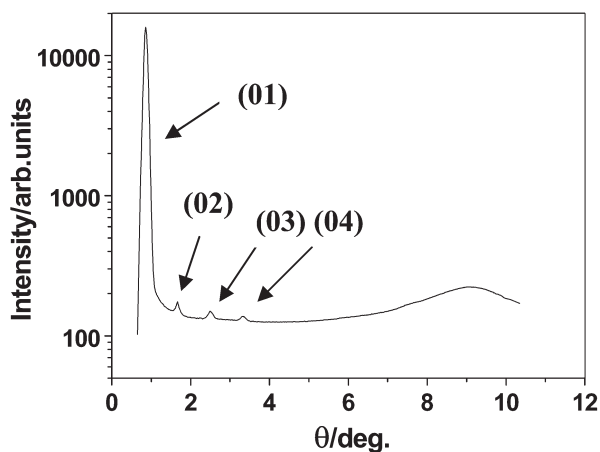

Figure 8. X-ray angular intensity profile obtained for the mesophase of compound **18** at 150°C, indicating a lamellar ordering of the molecules.

behaviour. A sample of this compound was taken in a cell made from ITO-coated glass plates which were treated for homogeneous alignment. The cell thickness was measured to be 8.5 μm. On very slow cooling of the isotropic liquid under a d.c. electric field of about 50 V, the mesophase appeared as circular domains in which the extinction cross made an angle with respect to the directions of the crossed polarizers as observed under a polarizing microscope. On reversing the polarity of the applied field, the domains with the extinction cross rotating in a clock-wise direction now rotated in an anticlock-wise direction and *vice versa*. On switching off the electric field (0 V), the extinction cross obtained in these circular domains reoriented along the directions of the crossed polarizers. As an example, consider the domains I and II in figures 9(*a–c*): in the absence of the electric field (0 V), the extinction cross obtained orients along the directions of the crossed polarizers as shown in figure 9(*a*). On application of an electric field, figure 9(*b*), the extinction cross in domain I, rotates in an anticlockwise direction while that in domain II rotates in a clockwise direction with respect to the crossed polarizers. This clearly suggests the existence of chiral domains of opposite handedness. On reversing the polarity of the applied field, these chiral domains switch to the other ferroelectric state. The dark extinction cross obtained at zero electric field, figure 9(*a*), is evidence for anticlinic ordering of the bent-core molecules in adjacent layers in these circular domains. At a saturated applied d.c. field, the domains in (*b*) and (*c*) exist in a synclinic ferroelectric state (SmC_SP_F) and these are chiral states. The maximum optical tilt angle estimated is about 36°. The field-induced chiral ferroelectric states (*b*) and (*c*) show different colours; this is due to unsymmetrical switching, i.e. the optical rotation for one sign of the field is different from the other.

A schematic representation of the arrangement of molecules in adjacent layers in each domain, that are responsible for the occurrence of heterochiral domains (opposite polarity and tilt), are also shown in figure 9. Interestingly, the dark brushes obtained rotate linearly (electroclinic effect) from SmC_AP_A state to SmC_SP_F state on increasing the d.c. electric field with saturation at $6\,V\,\mu m^{-1}$. However, no bistabilty could be observed in this mesophase even for a reduced cell thickness of about 4.5 μm, and the dark brushes always relax on turning off the applied field. Racemic ground state domains could also be seen in which the dark brushes exist along the directions of the crossed polarizers. No change in the position of the dark brushes was observed either by reversing the polarity of the applied field or in the absence of the field, as shown in figure 10. These observations suggest that these domains must be a
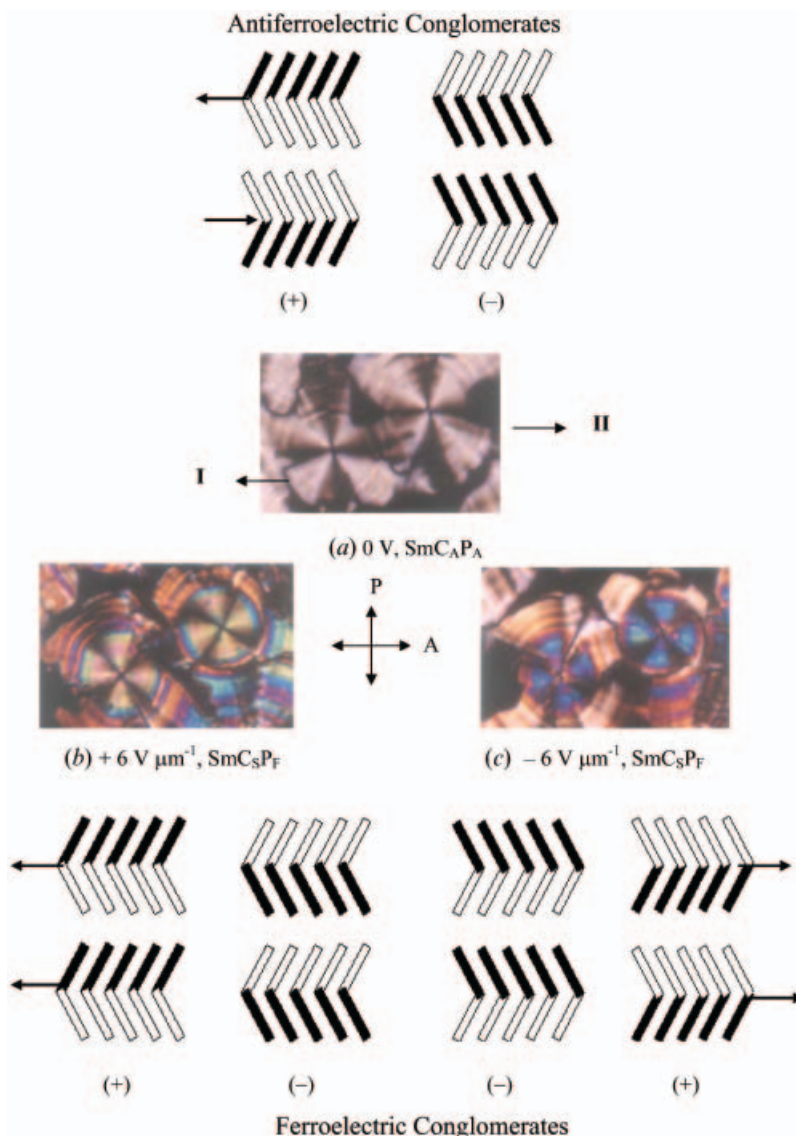
Antiferroelectric Conglomerates

(+)   (−)

(*a*) 0 V, SmC$_A$P$_A$

(*b*) + 6 V μm^{-1}, SmC$_S$P$_F$ (*c*) − 6 V μm^{-1}, SmC$_S$P$_F$

(+)   (−)   (−)   (+)

Ferroelectric Conglomerates

Figure 9.   Focal-conic circular domains of opposite handedness (**I, II**) obtained under a polarizing microscope for the mesophase of compound **16**. (*a*) 0 V, (*b*) + 6 V μm^{-1} and (*c*) − 6 V μm^{-1}. A schematic representation of the molecular organization (tilt and polarity) in such heterochiral domains exhibiting tristable switching is also presented. The solid segment of the BC molecules represents the orientation above the plane and the other segment is below the plane. The (+) and (−) signs indicate the opposite handedness.

mixture of domains with opposite tilt directions. The distance between the stripes indicates the size of the domains with alternating tilt.

These observations explain the occurrence of different mesophase structures on cooling the isotropic liquid. For example, on slow cooling the isotropic liquid, the long filaments obtained collapse directly to a more birefringent texture suggesting a racemic structure (synclinic tilt of molecules in adjacent layers). The observation of helical filaments indicates the chiral nature of the mesophase.

More interestingly, the colour changes with variation

of the d.c. field, as shown in figure 11, and this was found to be reversible. The colour of the texture changes gradually from purple red (2 V μm^{-1}) to green (6 V μm^{-1}) via violet (4 V μm^{-1}) on increasing the electric field. This indicates an increase in birefringence on increasing the applied field and such a behaviour has been observed by Walba *et al.* [20]. The stripes obtained over the fan-shaped texture exist parallel to the smectic layers, and are retained even at higher d.c. electric field.

As shown in figure 3, on cooling the isotropic liquid of compound **16** and viewing under a polarizing microscope, some circular domains were obtained in

Figure 10. Photomicrographs showing (*a*) the racemic ferroelectric state obtained in the B_{2X} phase of compound **16** by application of a d.c. field ($\pm 10\,V\,\mu m^{-1}$), and (*b*) the texture obtained on turning off the electric field, indicating the racemic nature of the domains. Note that the dark brushes obtained exist along the directions of the crossed polarizers.

which the dark brushes make an angle with respect to the directions of the crossed polarizers (for example domains 2 and 3). At lower voltages no effect could be observed. However, at high electric fields ($>5\,V\,\mu m^{-1}$) the dark brushes rotate along the orientation directions of the crossed polarizers. No switching could be observed on reversing the polarity of the electric field. On turning off the electric field the dark brushes remain unchanged as shown in figure 10 (*a*). This indicates the existence of synclinic-antiferroelectric (SmC_SP_A) ground state racemic domains. Under the electric field a racemic anticlinic-ferroelectric state (SmC_AP_F) is produced and is stabilized by the surface. In any case, the anticlinic ferro- and anticlinic antiferroelectric structures are stabilized under these conditions. On applying an electric field to the domains of type 1 (domain 1 in figure 3), only a few show a tristable switching indicating their chiral nature, and the remaining are racemic.

3.3. *Triangular-wave electric field studies*

Triangular-wave electric field experiments were carried out in order to confirm the antiferroelectric ground state and also to measure the polarization value for the mesophase of the same compound **16**. The sample was taken in a 10 μm thick cell as described above for d.c. field experiments. On application of a triangular-wave electric field of about $\pm 75\,V$ (threshold voltage is about $\pm 50\,V$) and at a frequency of 50 Hz, a broad single polarization current peak was observed for each half-cycle indicating a ferroelectric-type switching behaviour for the mesophase. The polarization current peak obtained completely disappears in the isotropic phase and reappears on cooling. This clearly confirms that the polarization peak is not due to ionic impurities or the cell. The calculated polarization value was about $490\,nC\,cm^{-2}$ and the current response trace obtained is shown in figure 12 (*a*). However, when a modified triangular-wave voltage was applied under these circumstances, the single polarization current peak

gave rise to two peaks indicating inherent antiferro-electric behaviour. On increasing the voltage further, at a second threshold voltage of about $\pm 110\,V$, a second polarization current peak appeared; the origin of the peak is shown by an arrow in figure 12 (*b*). This is the signature for the antiferroelectric ground state of the mesophase. The polarization value obtained by integrating the area under the two current peaks was about $885\,nC\,cm^{-2}$. The resultant triangular-wave current response is shown in figure 12 (*b*). On increasing the voltage further, the maximum polarization value that could be obtained was about $1000\,nC\,cm^{-2}$. This high polarization value is attributed to the presence of the polar cyano group, whose dipole is along the direction of the polar axis. The optical photomicro-graphs obtained at zero field, as well as after the first and the second threshold voltages, are shown in figure 13. It can be seen that at zero electric field, a striped pattern could be observed and at the first threshold voltage, part of this pattern disappears. At higher voltages, these stripes completely disappear leaving a smooth fan-shaped texture. This complicated and peculiar switching behaviour suggests a strong surface influence on the existence of the mesophase. Since this compound has a highly polar cyano group along the direction of the polar axis, its influence on the surface can be high.

3.4. *Influence of the position of fluorine substituent (series I and II)*

The two homologous series of compounds differ from one another by the position of the fluorine substituent. This strongly influences the transition temperatures, especially the melting point and also the stability of both mesophases. When a fluorine is substituted at the *meta*-position with respect to the carboxylate group on the middle phenyl ring (series **II**) of the arms of the bent-core, both melting and clearing temperatures are reduced and the thermal range of the mesophase increases in comparison with the other series
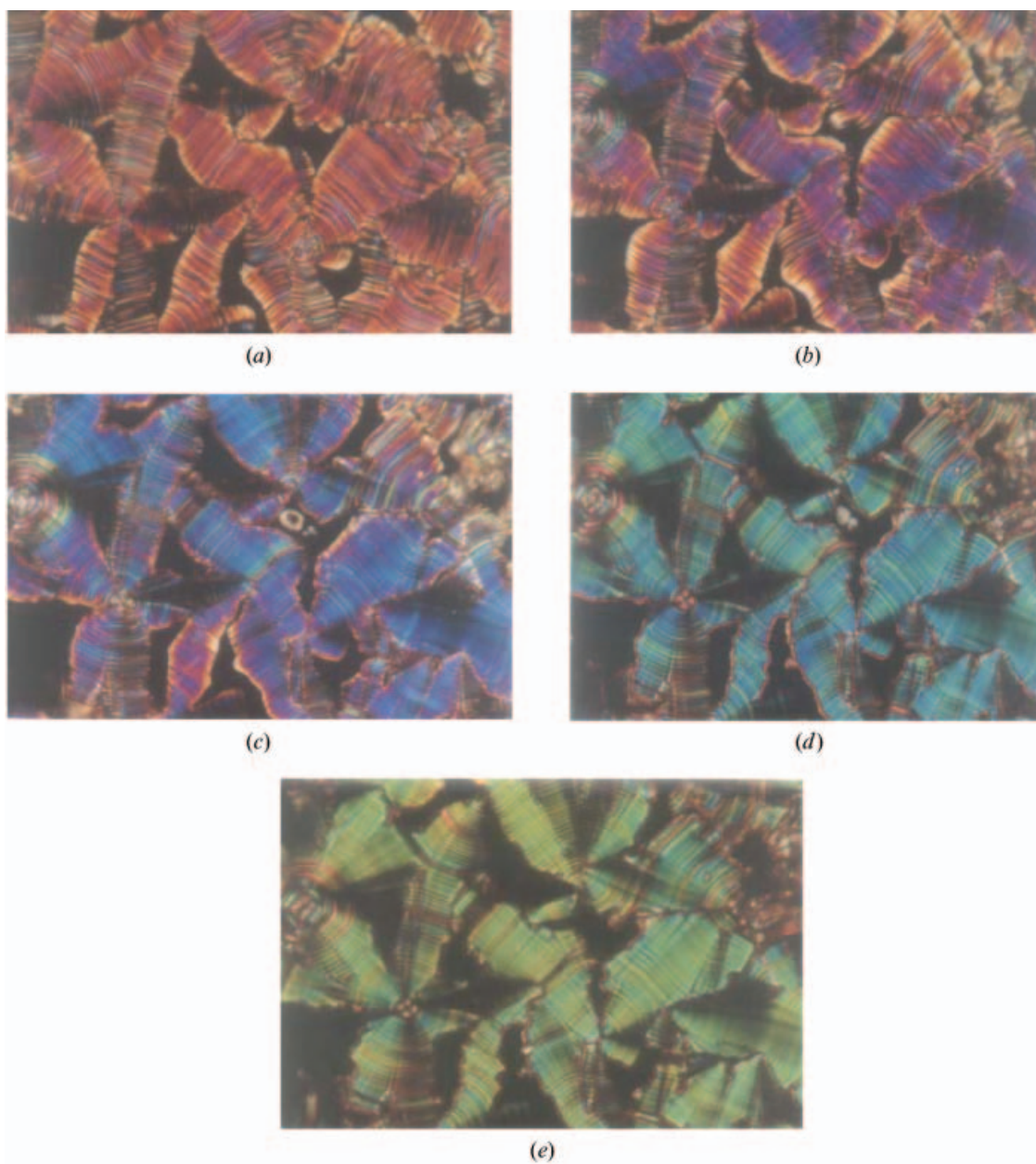
Figure 11. Photomicrographs of the mesophase of compound **16** showing change in colour with the variation of a d.c. field (increasing voltage). (*a*) $2\,V\,\mu m^{-1}$, purple-red; (*b*) $3\,V\,\mu m^{-1}$, dark violet; (*c*) $4\,V\,\mu m^{-1}$, blue and violet; (*d*) $5\,V\,\mu m^{-1}$, cyanish blue; (*e*) $6\,V\,\mu m^{-1}$, yellowish green.

I compounds. The B_1 mesophase is stabilized even for the higher homologues (compounds **13**–**15**) if a fluorine is at the *meta*-position (series **II**). The stability of the individual mesophases also depends on the orientation direction of the polar fluorine substituent with respect to the polar axis.

A plot of the melting and clearing temperatures as a function of *n*-alkyl chain length for the homologues of series **I** is shown in figure 14 (*a*). A steep decreasing trend is observed for the B_1–I phase transition while the B_{2X}–I curve is almost horizontal. The melting points increase for shorter chain length compounds on ascending the homologous series **I**, and hence the mesophase is completely suppressed for the middle homologues. For example, compound **5** does not show a mesophase and this is a cross-over homologue, where the lower homologues exhibit a B_1 phase and the higher homologues show a B_{2X} mesophase as shown in figure 14 (*a*). Similar trends could be observed for the homologues of series **II**, but the effect is minimal as
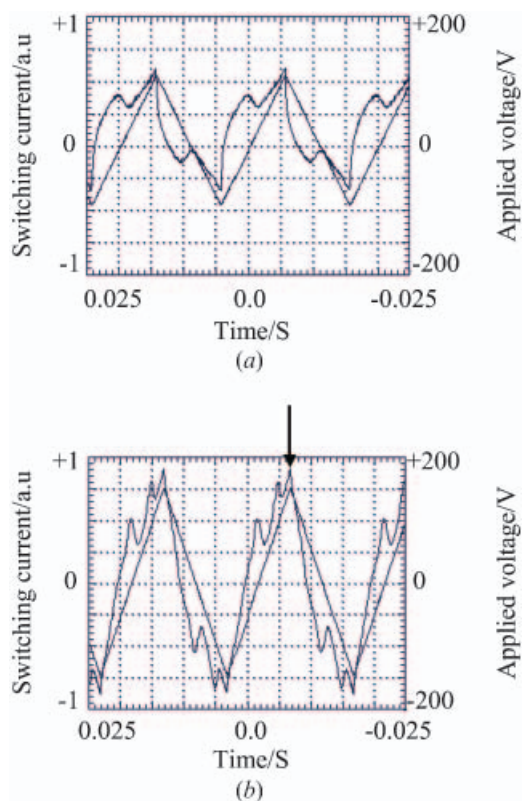
Figure 12. Switching current response obtained for the mesophase exhibited by compound **16** by applying a triangular-wave voltage at 160°C. Cell thickness 10 μm; (a) ± 75 V, 50 Hz, $P_S \approx 490$ nC cm^{-2}; (b) ± 150 V, 50 Hz, $P_S \approx 885$ nC cm^{-2}.

shown in figure 14 (b). The B$_1$–I and B$_{2X}$–I transition point curves show similar trends in both series of compounds.

4. Conclusions

Two new homologous series of compounds containing a highly polar cyano group along the arrow axis of bent-core molecules are reported. The mesophase obtained for higher homologues of both series shows a mixture of four different possible structures. Among these, two are chiral conglomerates with opposite tilt and polarity. The remaining two are racemic structures which arise from a synclinic tilt of BC molecules in adjacent layers in one case, and in the other a synclinic tilt of molecules in adjacent layers forming two different domains, which alternate. The observation of tristable switching, as well as two half-period polarization current peaks, confirms the ground state antiferroelectric structure for the mesophase. The spontaneously formed helical filaments and the chiral circular domains with helical periodicity suggest a structure for this mesophase that is different from a B$_2$
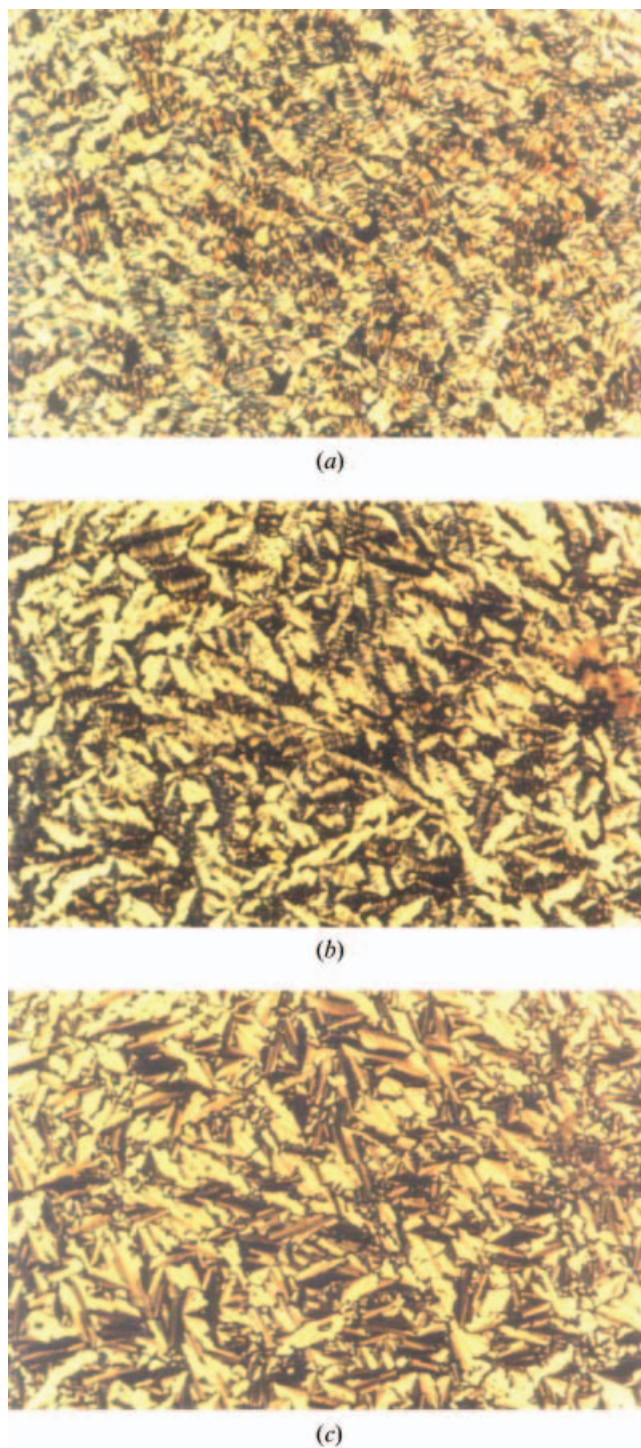

Figure 13. The change in textural pattern observed on application of a triangular-wave electric field of (a) 0 V, (b) ± 75 V, 50 Hz (above the first threshold voltage), and (c) ± 150 V, 50 Hz (above the second threshold voltage) for compound **16**.

phase. However, further experiments are required to understand the peculiar behaviour of this mesophase. It is also appropriate to mention here that, very recently,
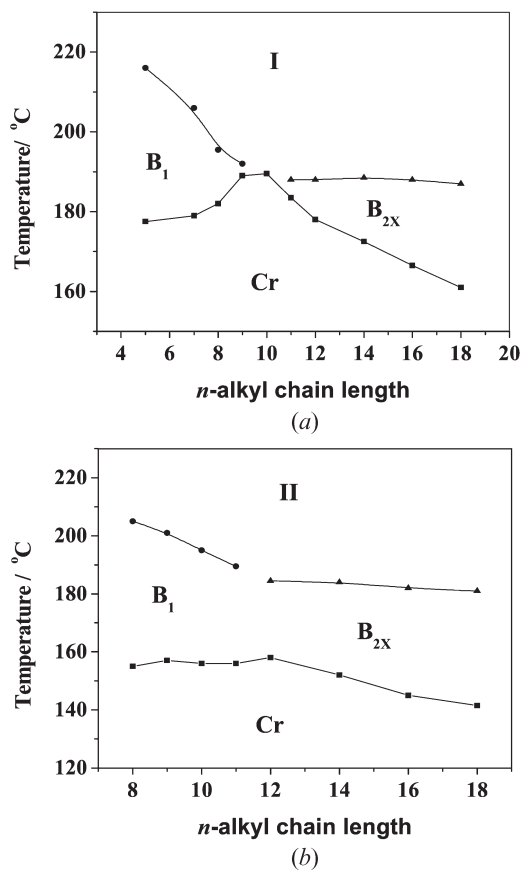
Figure 14. Plots of transition temperature as a function of the number of carbon atoms in the *n*-alkyl chain obtained for (*a*) series **I** and (*b*) series **II**.

Coleman *et al.*, [27] have carried out extensive and sophisticated experiments to solve the structure of mesophases exhibiting helical structures. Many of the optical textures exhibited by the B_{2X} phase are similar to those of the B_7 phase described in [27], although our X-ray diffraction studies suggest a simple B_2 phase structure.

References

[1] NIORI, T., SEKINE, T., WATANABE, J., FURUKAWA, T., and TAKEZOE, H., 1996, *J. mater. Chem.*, **6,** 1231.
[2] LINK, D. R., NATALE, G., SHAO, R., MACLENNAN, J. E., CLARK, N. A., KORBLOVA, E., and WALBA, D. M, 1997, *Science*, **278,** 1924.
[3] PELZL, G., DIELE, S., and WEISSFLOG, W., 1999, *Adv. Mater.*, **11,** 707.
[4] WALBA, D. M., KORBLOVA, E., SHAO, R., MACLENNAN, J. E., LINK, D. R., GLASER, M. A., and CLARK, N. A., 2000, *Science*, **288,** 2181.
[5] BEDEL, J. P., ROUILLON, J. C., MARCEROU, J. P., LAGUERRE, M., NGUYEN, H. T., and ACHARD, M. F., 2001, *Liq. Cryst.*, **28,** 1285.
[6] PRATIBHA, R., MADHUSUDANA, N. V., and SADASHIVA, B. K., 2000, *Science*, **288,** 2184.
[7] HEGMANN, T., KAIN, J., DIELE, S., PELZL, G., and TSCHIERSKE, C., 2001, *Angew. Chem. int. Ed.*, **40,** 887.
[8] EREMIN, E., DIELE, S., PELZL, G., NADASI, H., WEISSFLOG, W., SALFETNIKOVA, J., and KRESSE, H., 2001, *Phys. Rev. E.*, **64,** 051707.
[9] AMARANATHA REDDY, R., and SADASHIVA, B. K., 2004, *J. mater. Chem.*, **14,** 310.
[10] AMARANATHA REDDY, R., and SADASHIVA, B. K., 2003, *Liq. Cryst.*, **30,** 273; SHREENIVASA MURTHY, H. N., and SADASHIVA, B. K., 2003, *Liq. Cryst.*, **30,** 1051.
[11] BEDEL, J. P., ROUILLON, J. C., MARCEROU, J. P., LAGUERRE, M., NGUYEN, H. T., and ACHARD, M. F., 2000, *Liq. Cryst.*, **27,** 1411.
[12] LEE, C. K., PRIMAK, A., JAKLI, A., CHOI, E. J., ZIN, W. C., and CHIEN, L. C., 2001, *Liq. Cryst.*, **28,** 1293.
[13] JAKLI, A., NAIR, G. G., LEE, C. K., SUN, R., and CHIEN, L. C., 2001, *Phys. Rev. E.*, **63,** 061710.
[14] HEPPKE, G., PARGHI, D. D., and SAWADE, H., 2000, *Liq. Cryst.*, **27,** 313.
[15] DE GENNES, P. G., 1975, *The Physics of Liquid Crystals* (Oxford: Clarendon Press).
[16] BRAND, H. R., CLADIS, P. E., and PLEINER, H., 1998, *Eur. Phys. J. B*, **6,** 347.
[17] JAKLI, A., KRUERKE, D., SAWADE, H., and HEPPKE, G., 2001, *Phys. Rev. Lett.*, **25,** 5715.
[18] JAKLI, A., NAIR, G. G., SAWADE, H., and HEPPKE, G., 2003, *Liq. Cryst.*, **30,** 265.
[19] EREMIN, E., DIELE, S., PELZL, G., NADASI, H., and WEISSFLOG, W., 2003, *Phys. Rev. E.*, **67,** 021702.
[20] WALBA, D. M., KORBLOVA, E., SHAO, R., and CLARK, N. A., 2001, *J. mater. Chem.*, **11,** 2743.
[21] WEISSFLOG, W., LISCHKA, C., BENNE, I., SCHARF, T., PELZL, G., DIELE, S., and KRUTH, H., 1998, *Proc. SPIE*, **3319,** 14.
[22] WEISSFLOG, W., NADASI, H., DUNEMANN, U., PELZL, G., DIELE, S., EREMIN, A., and KRESSE, H., 2001, *J. mater. Chem.*, **11,** 2748.
[23] JUNCAI, F., BIN, L., YANG, L., and CHANGCHUAN, L., 1996, *Synth. Commun.*, **26,** 4545.
[24] AMARANATHA REDDY, R., and SADASHIVA, B. K., 2000, *Liq. Cryst.*, **27,** 1613.
[25] SADASHIVA, B. K., and SUBBA RAO, G. S. R., 1977, *Mol. Cryst. liq. Cryst.*, **38,** 703.
[26] PALFFY-MUHORAY, P., BERGERSEN, B., LIN, H., MEYER, R. B., and RACZ, Z., 1992, in *Pattern Formation in Complex Dissipative Systems*, edited by S. Kai (World Scientific), p.504.
[27] COLEMAN, D. A., FERNSLER, J., CHATTHAM, N., NAKATA, M., TAKANISHI, Y., KORBLOVA, E., LINK, D. R., SHAO, R. F., JANG, W. G., MACLENNAN, J. E., MONDAINN-MONVAL, O., BOYER, C., WEISSFLOG, W., PELZL, G., CHIEN, L. C., ZASADZINSKI, J., WATANABE, J., WALBA, D. M., TAKEZOE, H., and CLARK, N. A., 2003, *Science*, **301,** 1204.